UCSF
UC San Francisco Previously Published Works

Title
Quadrupole mass spectrometry desorption analysis of Ga adsorbate on AlN (0001)

Permalink
https://escholarship.org/uc/item/61w8b5th

Journal
Journal of Vacuum Science & Technology A, 24(6)

ISSN
0734-2101

Authors
Brown, J S
Koblmuller, G
Averbeck, R
et al.

Publication Date
2006-11-01

Peer reviewed

eScholarship.org Powered by the California Digital Library
University of California

Quadrupole mass spectrometry desorption analysis of Ga adsorbate on AlN (0001)

Jay S. Brown and Gregor Koblmüller
Materials Department, University of California, Santa Barbara, California 93106-5050

Robert Averbeck and Henning Riechert
Infineon Technologies AG, Corporate Research Photonics, D-1730 Munich, Germany

James S. Speck[a)]
Materials Department, University of California, Santa Barbara, California 93106-5050

(Received 1 December 2005; accepted 25 July 2006; published 10 October 2006)

The authors have investigated the adsorption and subsequent desorption of Ga on AlN (0001) with line-of-sight quadrupole mass spectrometry (QMS). The authors present desorption data consistent with a continuous Ga-flux dependent accumulation of a laterally contracted Ga bilayer on AlN (0001) from 0 to 2.7±0.3 ML GaN equivalent coverage, and further Ga accumulation in macroscopic Ga droplets. The temperature dependence of Ga-adsorbate QMS desorption transients was investigated and the authors determined that the desorption activation energies for individual monolayers of the Ga adsorbate on AlN (0001) were similar to Ga desorption from GaN (0001). For the (first) pseudomorphic Ga-adsorbate monolayer on AlN, the authors measured a maximum Ga coverage of 1.0±0.1 ML and desorption activation energy of 6.2±0.3 eV. For the (second) laterally contracted Ga monolayer (1.7±0.3 ML) the desorption activation energy was 3.8±0.1 eV. © *2006 American Vacuum Society.* [DOI: 10.1116/1.2338554]

I. INTRODUCTION

High Al-content III-nitride semiconductor heterostructures have been the subject of intense study due to a variety of applications such as ultraviolet III-nitride light emitting diodes,[1–3] as well as GaN-based high electron mobility transistors.[4,5] Improved fundamental understanding of the growth of AlN by rf plasma assisted molecular beam epitaxy (PA-MBE) is necessary for further improvement of interfaces in heterostructures.[6,7] Under conditions similar to AlN growth by MBE, the stability of a laterally contracted Al bilayer has been predicted by first principles calculations and directly observed by scanning tunneling microscopy.[8,9] In both Ga/GaN (Ref. 10) and Al/AlN,[8] the first monolayer of adsorbate metal has been proposed to be pseudomorphic to the underlying wurtzite structure and the second metal adsorbate monolayer has been found to be laterally contracted (LC) with GaN (AlN) equivalent coverage of 1–2 ML. In the case of Ga/GaN, the LC monolayer has been found to be an incommensurate fluid with respect to the underlying substrate at temperatures above 200 °C, while the Al adsorbate retains hexagonal symmetry and shows surface reconstructions at growth temperatures (up to 850 °C).[9] Under conditions similar to GaN homoepitaxy by PA-MBE, calculations of N diffusion on the bare GaN (0001) surface and within the Ga-adsorbate bilayer have indicated that the Ga-adsorbate bilayer provides a lower energy barrier to surface diffusion.[11] Recent experiments, using line-of-sight quadrupole mass spectrometry (QMS), have demonstrated a continuously increasing Ga-adsorbate coverage[12,13] and improved surface morphology[14,15] for GaN growth with increasing Ga flux.

During AlN-based GaN heterostructure growth by PA-MBE, GaN quantum wells (QWs) or quantum dots (QDs), the presence of a Ga adsorbate on the AlN surface during GaN growth initiation has been recognized as crucial in the mediation of growth mode and adatom surface mobility.[16] The presence of a dynamically stable Ga adlayer on AlN during GaN growth was reported to result in step-flow morphology and to prevent the partial elastic relaxation during Stranski-Krastanov (SK) transition, which provided a viable route to QW growth.[17] In the growth of GaN QDs on AlN (0001) by PA-MBE, further reports have clarified the importance of excess Ga flux in determining GaN growth mode on AlN. Under N-rich growth conditions, the initial GaN growth mode on AlN was found to be layer by layer, and the SK transition occurred after 2–3 ML GaN deposition, consistent with previous reports of the SK growth mode in other material systems.[18] However, under Ga-rich flux conditions, desorption of the Ga adsorbate preceded the SK transition, which has been referred to as "Ga-autosurfactant modified" SK GaN growth.[17,19] A comparison of the size and density for both types of GaN QDs, grown under SK (Ref. 8) and modified SK (Refs. 17 and 19) conditions, is consistent with reduced adatom mobility under zero Ga-adsorbate coverages as compared to finite coverages (2–3 ML) predicted by the theory.[11] Under modified SK (Refs. 17 and 19) conditions, GaN QDs are relatively larger and of lower areal density[12] than GaN QDs grown under conventional SK (Ref. 18) conditions.

In light of recent experiments[12–15] and the importance of the Ga adsorbate in the mediation of GaN growth on AlN,[16–19] we have investigated the structure and kinetics of the Ga adlayer on AlN (0001) by performing Ga adsorption

[a)]Electronic mail: speck@mrl.ucsb.edu

with AlN (0001) substrate temperatures similar to those used during PA-MBE growth of GaN/AlN heterostructures. In the following sections, we present experimental evidence for the presence of a LC Ga adlayer on AlN (0001).

II. EXPERIMENT

In this work, growth of AlN (0001) on SiC and subsequent Ga adsorption experiments were carried out in a VH80 (VG Semicon) reactor equipped with standard Ga and Al effusion cells and radio frequency plasma source (EPI). The substrate temperature was controlled by thermocouple located inside the substrate heater. The wafer surface temperature was monitored directly by a normal incidence emissivity corrected (0.63) pyrometer with maximum sensitivity at 940 nm. Routine growth of GaN by PA-MBE under excess metal conditions results in a gradual accumulation of metal on the pyrometer window and leads to observable pyrometer temperature changes, depending on growth temperatures and excess fluxes, because of absorption losses. Prior to the adsorption experiments described below, we calibrated the pyrometer temperature response by comparison of the substrate temperature at Ga-droplet formation for known Ga flux.[12,20] All pyrometer temperatures reported in this work are based upon the calibration of pyrometer response at 743 °C, 20 nm/min Ga flux.[12]

The group-III fluxes were measured by cross sectional scanning electron microscopy (SEM) imaging of metal flux-limited 1–2 μm films grown on SiC. The SEM growth rate measurements were used to calibrate the beam flux monitor (ion gauge) measurements, and we calibrated the fluxes to effusion cell temperature prior to all measurements.

We calibrated the linear response of the line-of-sight QMS detector by adsorption of Ga fluxes (1–30 nm/min) on a 50.8 mm diameter sapphire wafer at a temperature of 804 °C. As previously described,[12,13] Ga adatoms have a negligible surface residence time under these adsorption conditions and we observed steady-state desorption Ga fluxes that were directly dependent on incident Ga flux.[12,13]

As previously described, ~225 nm AlN (0001) was grown by PA-MBE on 50.8 mm diameter 6*H*-SiC (0001) wafers under Al-rich intermediate (3.25 nm/min Al flux) conditions at 784 °C, with N-limited AlN growth rate of 2.5 nm/min.[21] After AlN growth, the excess Al was consumed by exposure to N flux for 15 min at 784 °C. During exposure to the N flux, the AlN surface was monitored by the reflection high energy electron diffraction (RHEED) specular intensity, and evolution of the two-dimensional diffraction pattern.[22] In general, the AlN RHEED pattern intensity increased and became more diffuse during N-flux exposure, indicative of the incorporation of excess Aluminum.

Two classes of Ga adsorption experiments on AlN (0001) were performed by changing the incident Ga flux with fixed substrate temperature and by changing the substrate temperature with fixed Ga incident flux. These studies were designed to follow the analysis of Ga on GaN (0001) and GaN ($000\bar{1}$) by Koblmüller *et al.*[13]

A. Variable Ga-flux adsorption on AlN (0001)

The incident Ga flux was varied from 1 to 20 nm/min, with 30 s Ga adsorption with each Ga flux at a substrate temperature of 672±2 °C. After each adsorption wetting pulse, the Ga shutter was closed to allow adsorbed Ga to desorb from the AlN (0001) surface under vacuum. The Ga effusion cell temperature was stabilized for at least 8 min prior to each wetting experiment.

B. Temperature dependence of Ga desorption from AlN (0001)

Adsorption on AlN (0001) with a Ga flux sufficient for Ga droplet formation[20] with substrate temperatures in the range of 634–704 °C, with incremental temperature changes of 5±1 °C was performed. In each case, a total Ga fluence of 8 ML was deposited with a Ga flux of 3.9 nm/min (0.25 ML/s). The substrate temperature was stabilized for 4 min after complete desorption of the Ga adsorbate from the AlN (0001) surface under vacuum prior to each adsorption experiment. This experiment was used to assess the temperature variation of the mean adatom lifetimes according to the bilayer desorption model presented for Ga on GaN (0001).[13]

III. RESULTS

A. Variable Ga-flux adsorption on AlN (0001)

We first discuss the salient features of an individual Ga adsorption wetting pulse on AlN (0001) at 672 °C. Distinct time intervals of the temporal Ga-desorption flux were integrated to determine the Ga-adsorbate coverage on AlN (0001), in accordance with the LC Ga bilayer desorption characteristic that has been observed on GaN (0001).[13] We compared the saturation of desorption Ga flux with respect to incident Ga flux to the case of Ga-droplet desorption on GaN (0001), and we attribute the steady-state desorption flux after Ga adsorption on AlN (0001) to Ga-droplet desorption.

Typical QMS data are shown in Fig. 1 a for 30 s Ga adsorption with 6 nm/min incident flux on AlN (0001). The initiation of Ga adsorption is evidenced by an abrupt increase in desorption Ga flux from the detection limit to an adsorption steady state. After the Ga shutter was closed, the steady-state Ga desorption flux provided a direct indication that Ga droplets were formed on the surface during adsorption.[12,13] The steady-state desorpiton of Ga under vacuum is consistent with adsorption from the two-dimensional adsorbate surface, which is maintained near full coverage by diffusion from a Ga-droplet reservoir, as shown schematically in Fig. 2(a). For comparison, a 1 nm/min Ga-flux adsorption pulse is depicted in Fig. 1(b), in which Ga droplets did not form and immediate desorption flux decay was observed after Ga-shutter closure, as shown in the schematic for PM monolayer desorption in Fig. 2(d).

Assessment of Ga-adsorbate coverage corresponding to incident Ga flux was realized by integration of QMS data as indicated by the shaded and hatched regions in Fig. 1. Similar to the case of the Ga-adsorbate accumulation on GaN (0001),[12,13] the total Ga-adsorbate coverage on AlN (0001),

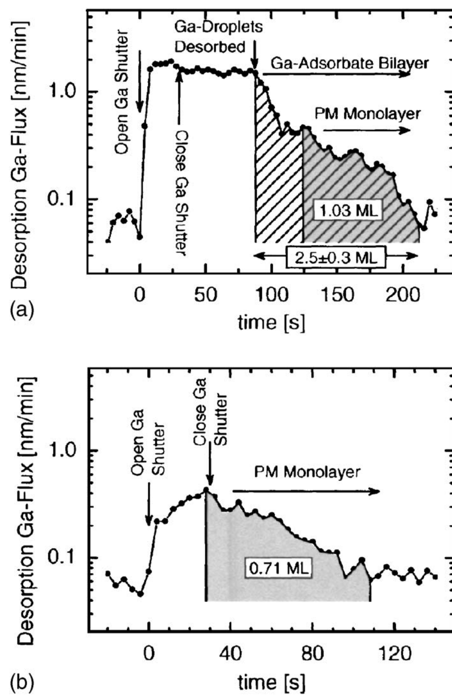

FIG. 1. Typical line-of-sight quadrupole mass spectrometry desorption flux measurements of ^{69}Ga during and after 30 s Ga adsorption on AlN (0001) with substrate temperature of 672±2 °C. The hatched and shaded regions indicate integration of desorption Ga flux for the determination of the LC and PM monolayer coverages, respectively. (a) Adsorption with 6 nm/min Ga flux. Subsequent steady-state Ga-droplet desorption and a 2.46 ML Ga bilayer. (b) Adsorption with 1 nm/min Ga flux. Subsequent desorption of an incomplete PM monolayer, 0.71 ML Ga-adsorbate coverage.

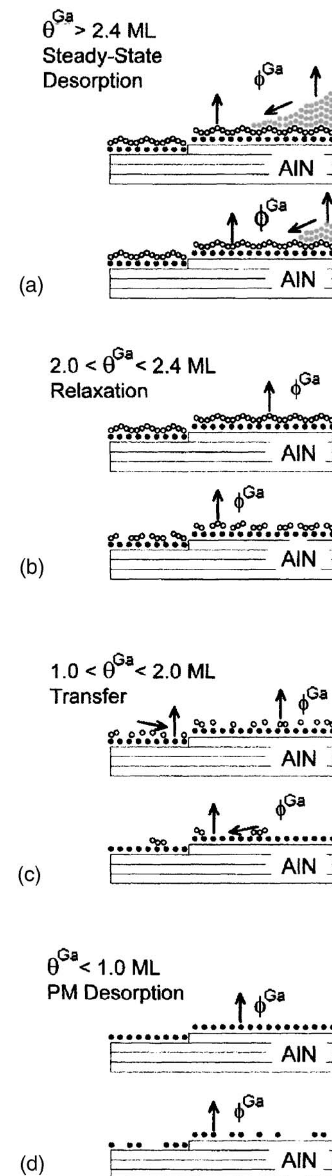

FIG. 2. Desorption schematic sequence of adsorbed Ga droplets and Ga bilayer on AlN (0001) [see Ref. 13 for further details regarding Ga on GaN (0001) surfaces]. Black circles represent Ga atoms in the PM monolayer, open circles represent Ga atoms in the LC monolayer, and solid gray circles represent Ga atoms in liquid droplets. (a) Steady-state desorption is observed while Ga droplets remain on the surface and the total adsorbate coverage is greater than ~2.4 ML. Desorption flux is dominated by the LC Ga-adsorbate monolayer, and the Ga droplets maintain the LC monolayer at full coverage via surface diffusion. (b) In the *relaxation* stage, the total Ga-adsorbate coverage is between ~2.4 and 2.0, the desorption flux evidences exponential decay from the steady-state level while desorption is dominated by the LC monolayer. (c) During the *transfer* stage, the total Ga-adsorbate coverage is between 2.0 and 1.0, the desorption flux is momentarily at a steady-state level while the PM monolayer is maintained at 1.0 ML by surface diffusion from the LC monolayer. (d) When the total coverage is 1.0 ML, the desorption flux from the PM monolayer decays exponentially to the background detection limit.

determined by integration of desorption Ga flux after the Ga shutter was closed, was observed to continuously increase with increasing incident Ga flux (Fig. 3). For all desorption Ga-flux transients with Ga fluxes greater than 2.5 nm/min resulting in Ga-adlayer completion and Ga-droplet formation at 672 °C, we integrated the desorption flux from the onset of desorption transient decay (nearest data point) which resulted in an Ga-adsorbate coverage of 2.7±0.3 ML. As shown in Fig. 3, it is apparent that the measured decay coverage increased minimally beyond the critical Ga flux for Ga-droplet formation. We note that near the critical Ga flux (2.5 nm/min) the integrated decay coverage was found to be in the range of 1.99–2.46 ML, an average of 2.2±0.2 ML, which is close to the predicted Ga bilayer on GaN coverage of 2.33 ML.[10] Sources of error in our measurements include the time resolution of QMS data (4 s), the ambiguity of determining the point of desorption flux decay in several instances, and nonuniformity across the wafer surface due to temperature and flux distribution. These sources of error are consistent with the large standard deviation (0.3 ML) obtained for the dataset of all decay coverages. It is also plausible that (unintentional) AlN roughness could have contributed to a higher than expected total bilayer coverage. However, previous experiments with Ga adsorption from GaN has indicated that GaN roughness was not a significant source of error in adsorbate coverage measurements.[13]

For each incident Ga-flux adsorption experiment, specific intervals of the distinct three-stage transient decay of desorption Ga flux were integrated as indicated in Fig. 1 to determine the Ga-adsorbate coverage corresponding to the three-

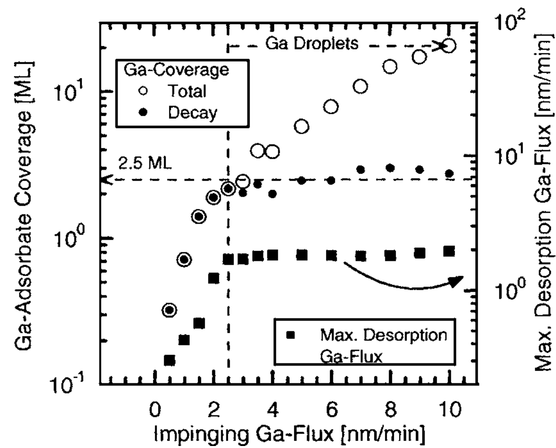

FIG. 3. Dependence of the total decay (two dimensional) Ga coverage, and maximum Ga desorption flux on the incident Ga flux from AlN (0001) (672 °C substrate temperature).

stage model for bilayer desorption.[13] In the analysis of Ga on GaN, up to a measured Ga adsorbate coverage of 1.0 ML, a single exponential (linear on semilog scale) desorption flux decay was observed,[23] which was attributed to the desorption of a pseudomorphic monolayer (PM) on GaN (0001) as shown in Fig. 2(d).[13] Similarly, for Ga on AlN (0001), we integrated the desorption Ga flux for time intervals corresponding to the final single exponential flux decay for all of the variable Ga-flux adsorption experiments and determined the Ga-adsorbate coverage to be 1.0 ± 0.1 ML, similar to the PM monolayer in the Ga bilayer on GaN (0001).[13]

As shown in Fig. 3, the maximum steady-state Ga desorption flux increased with increasing incident Ga flux, up to the incident Ga flux at which the Ga droplets formed, approximately 2.5 nm/min. This saturation point corresponded to the Ga flux at which the Ga-adsorbate coverage reached 2.2 ± 0.2 ML. As shown in Fig. 3, the Ga-adsorbate coverage of the transient desorption flux decay, indicated by the hatched region in Fig. 1, did not increase significantly with respect to experimental error for all incident Ga fluxes above 2.5 nm/min. These results are consistent with the Ga adsorption and accumulation of a bilayer (2.2 ± 0.2 ML) and Ga droplets on GaN (0001).[13]

At the 672 ± 2 °C substrate temperature in the variable Ga-flux study on AlN (0001), the observed Ga-droplet desorption flux saturation value, 1.55 ± 0.07 nm/min, was consistent with a substrate temperature of 668–669 °C predicted by the Ga/GaN adsorption diagram, based upon the assumption that the saturation desorption flux corresponds to the maximum surface desorption flux.[12,20] This agreement provides an independent validation of our previously described pyrometer calibration at 743 °C, 20 nm/min Ga flux. We conclude that for total Ga coverage beyond the saturation of the two-dimensional 2.2 ± 0.2 ML Ga-adsorbate phase, the bulk liquid Ga-droplet phase was formed on the surface as shown by the schematic in Fig. 2(a). The variable Ga-flux experimental results are consistent with the preliminary conclusion that the excess Ga on the AlN (0001) surface that is accumulated beyond the 2.2 ± 0.2 ML bilayer is subject to its bulk liquid-Ga attraction, just as in the case of adsorbed Ga on GaN (0001).[12,13,20] The temperature dependent desorption kinetics, presented in the next section, help to further elucidate the similarities and differences between the desorption activation energies of the PM, LC, and Ga-droplet adsorbate phases on GaN and AlN (0001).

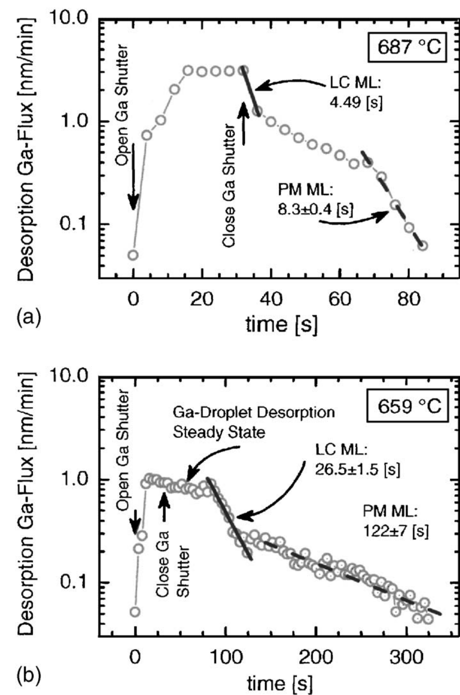

FIG. 4. Representative line-of-sight quadrupole mass spectrometry desorption flux measurements of ^{69}Ga during and after 8 ML Ga adsorption on AlN (0001). The solid and dashed lines indicate integration intervals of the total desorption transient used for determination of mean adatom lifetime (inset) for the LC and PM desorption Ga adsorbate phases, respectively. (a) Adsorption with 687 °C substrate temperature. (b) Adsorption with 659 °C substrate temperature.

B. Temperature dependence of Ga desorption from AlN (0001)

Temperature dependent experiments were performed to determine an apparent desorption activation energy for each of the monolayers of the Ga bilayer on AlN (0001). As shown in Fig. 4 for two substrate temperatures, 687 and 659 °C, desorption transient intervals corresponding to the Ga adsorbate coverage attributed to the LC monolayer and the PM monolayer were linear on a logarithmic flux scale versus desorption time t. This observation is consistent with the Ga-adsorbate bilayer desorption process proposed for the laterally contracted Ga bilayer on GaN (0001),[13] as shown schematically in Fig. 2. In the proposed desorption model the Ga-droplet phase and the LC and PM monolayers are depleted sequentially via desorption and surface diffusion, and corresponding intervals of the desorption transients may be used to extract an apparent desorption activation energy for each phase of the adsorbate. The decay of LC and PM desorption rates of Ga on AlN (0001), similar to the case of Ga on GaN (0001), was consistent with exponential desorption

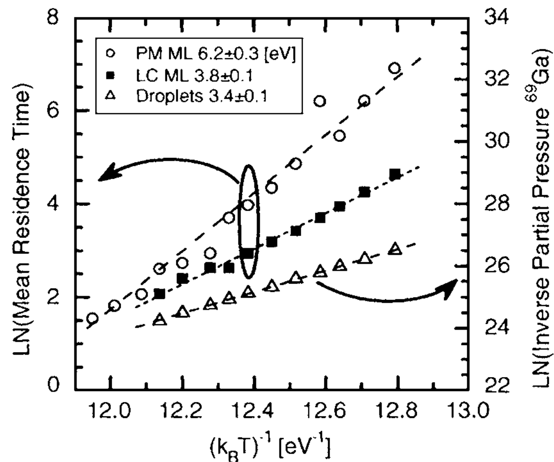

FIG. 5. Ga-adsorbate phase Arrhenius plots of mean adatom residence time and inverse partial pressure (proportional to inverse maximum Ga-desorption flux) used to determine the apparent desorption activation energies from temperature dependent line-of-sight quadrupole mass spectro metry measurements of Ga on AlN (0001).

rate processes, where the Ga surface population and total desorption flux is proportional to $\exp(-t/\tau_A)$. As indicated in Fig. 4, the mean adatom lifetimes τ_A were determine for both the LC and PM monolayers for each adsorption temperature. As previously described,[13] linear fits to Arrhenius plots of mean adatom lifetime versus thermal energy (Fig. 5) were used to determine apparent desorption activation energies E_A and desorption attempt prefactors υ_0 for the PM and LC Ga-adsorbate adlayers on AlN (0001), based upon the application of the Frenkel equation[24] for the temperature dependence of adatom lifetime, $\tau_A=(\upsilon_0)^{-1}\exp(E_A/k_BT)$. The mean adatom lifetime for steady-state desorption processes, such as the steady-state desorption attributed to the Ga-droplet phase, was taken to be inversely proportional to the desorption Ga flux.[13] The Ga-droplet steady-state desorption is indicated in Fig. 4(b) and is also apparent in Fig. 1(a). In Fig. 5, the temperature dependence of the Ga-droplet inverse steady-state desorption Ga flux is shown, along with the measured Ga-droplet desorption activation energy on AlN (0001) of 3.4±0.1 eV.

As shown in Fig. 5, we have measured increasing desorption activation energies for Ga-droplet phase of 3.4±0.1 eV, LC monolayer of 3.8±0.1 eV, and PM monolayer of 6.2±0.3 eV, which compares favorably with the Ga adsorption on GaN (0001) results reported by Koblmüller *et al.*[13] The Ga-droplet desorption activation energy on GaN, determined from separate QMS measurements on different GaN surfaces, was found to be 3.1±0.2.[13] The activation energy for the desorption of bulk liquid Ga has been reported to be 2.9 eV.[25] We note that in the case of relatively small Ga droplets on GaN or AlN surfaces, kinetic effects are likely to modify the activation energy from that observed from bulk Ga desorption. The LC monolayer desorption activation energy for Ga on GaN (0001) was found to be ~3.7 eV.[13] We note that while the LC and Ga-droplet activation energies for Ga on AlN (0001) are nearly the same as those for Ga on GaN (0001) within experimental error, the PM monolayer desorption activation energy was found in this work to be significantly larger for the Ga adsorbate on AlN (0001).[13] In the next section, we discuss the similarities and differences between desorption kinetics for the Ga bilayer on both AlN and GaN (0001) surfaces.

IV. DISCUSSION

For the Ga-adsorbate PM monolayer on AlN (0001) we measured a maximum Ga coverage of 1.0±0.1 ML and apparent desorption activation energy of 6.2 eV, that is greater than the 4.9 eV which was measured in the case of Ga on GaN (0001).[13] In contrast, the similar desorption activation energies for the LC Ga adlayer on both GaN and AlN (0001) are consistent with the conclusion that the Ga atoms within the LC monolayer are bound primarily to the Ga atoms in the PM monolayer.[10] This is in accord with the lateral contraction of the adlayer toward the bulk Ga lattice constant[10] and the corresponding observation of the higher atomic density, (1.4)±0.3 ML, in the LC adlayer on both surfaces. A similar argument may be made for the temperature dependent increase of Ga flux sufficient for Ga-droplet formation; in both GaN and AlN (0001) the Ga-droplet desorption activation energy is in the range of 3.1–3.4 eV. The activation energy for desorption in vacuum for bulk liquid Ga has been well established to be close to 2.9 eV over a wide range of temperatures.[25] In the present analysis of Ga on AlN (0001) we have applied a simplistic model for thermally activated desorption (single exponential behavior) to quantify the relative desorption behavior for the Ga-droplet phase and the LC and PM monolayers. This model may not be sufficient to describe the more detailed atomistic behavior, which is likely to be influenced by kinetic processes such as diffusion and multiple activation barriers to desorption.

V. SUMMARY AND CONCLUSIONS

We have demonstrated the presence of a laterally contracted (LC) Ga bilayer on AlN (0001) for substrate temperatures in the range of 634–704 °C. We have found that the phase-dependent desorption activation energies for the Ga adsorbate on AlN (0001) are similar to the Ga-adsorbate bilayer on GaN (0001), but that the first (PM) Ga-adsorbate monolayer is more tightly bound to the AlN surface than to the GaN surface. The conditions under which we have characterized the Ga bilayer on AlN (0001) are similar to GaN growth by PA-MBE, and we expect that enhanced surface diffusion of N adatoms[11] may be present during GaN growth on AlN.

We propose that the existence of a LC Ga bilayer on AlN (0001) has direct relevance for GaN heterostructure growth kinetics on AlN (0001) during PA-MBE, based upon previous results from experiment[13–15] and theory[11] for GaN growth. We have demonstrated that the Ga-adsorbate coverage may be controlled continuously from 0 to 2.7 ML, and we anticipate that this result could be used for the direct mediation of GaN growth kinetics during the Stranski-Krastanov transition of GaN on AlN (0001). Calculations of

the interfacial energy between several monolayers of GaN on AlN and a Ga bilayer could provide further insight into the Ga-adlayer mediated SK transition in GaN.

ACKNOWLEDGMENT

The authors gratefully acknowledge support from AFOSR (G. Witt, Program Manager).

[1]A. J. Fischer *et al.*, Appl. Phys. Lett. **84**, 3394 (2004).
[2]K. Iida *et al.*, J. Cryst. Growth **272**, 270 (2004).
[3]C. G. Moe *et al.*, Jpn. J. Appl. Phys., Part 2 **44**, L502 (2005).
[4]L. Shen *et al.*, J. Electron. Mater. **33**, 422 (2004).
[5]S. Rajan, P. Waltereit, C. Poblenz, S. J. Heikman, D. S. Green, J. S. Speck, and U. K. Mishra, IEEE Electron Device Lett. **25**, 247 (2004).
[6]D. Jena, A. C. Gossard, and U. K. Mishra, Appl. Phys. Lett. **76**, 1707 (2000).
[7]D. Jena, I. Smorchkova, A. C. Gossard, and U. K. Mishra, Phys. Status Solidi B **228**, 617 (2001).
[8]C. D. Lee, Y. Dong, R. M. Feenstra, J. E. Northrup, and J. Neugebauer, Phys. Rev. B **68**, 205317 (2003).
[9]R. M. Feenstra, Y. Dong, C. D. Lee, and J. E. Northrup, J. Vac. Sci. Technol. B **23**, 1174 (2005).
[10]J. E. Northrup, J. Neugebauer, R. M. Feenstra, and A. R. Smith, Phys. Rev. B **61**, 9932 (2000).
[11]J. Neugebauer, T. K. Zywietz, M. Scheffler, J. E. Northrup, H. Chen, and R. M. Feenstra, Phys. Rev. Lett. **90**, 056101 (2003).
[12]J. S. Brown, G. Koblmuller, F. Wu, R. Averbeck, H. Riechert, and J. S. Speck, J. Appl. Phys. **99**, 074902 (2006).
[13]G. Koblmuller, R. Averbeck, H. Riechert, and P. Pongratz, Phys. Rev. B **69**, 035325 (2004).
[14]G. Koblmueller, J. S. Brown, R. Averbeck, H. Riechert, P. Pongratz, and J. S. Speck, Jpn. J. Appl. Phys., Part 2 **44**, L906 (2005).
[15]G. Koblmuller, J. Brown, R. Averbeck, H. Riechert, P. Pongratz, and J. S. Speck, Appl. Phys. Lett. **86**, 041908 (2005).
[16]G. Mula, C. Adelmann, S. Moehl, J. Oullier, and B. Daudin, Phys. Rev. B **64**, 195406 (2001).
[17]C. Adelmann, N. Gogneau, E. Sarigiannidou, J. L. Rouviere, and B. Daudin, Appl. Phys. Lett. **81**, 3064 (2002).
[18]C. Adelmann, B. Daudin, R. A. Oliver, G. A. D. Briggs, and R. E. Rudd, Phys. Rev. B **70**, 125427 (2004).
[19]N. Gogneau, D. Jalabert, E. Monroy, T. Shibata, M. Tanaka, and B. Daudin, J. Appl. Phys. **94**, 2254 (2003).
[20]B. Heying, R. Averbeck, L. F. Chen, E. Haus, H. Riechert, and J. S. Speck, J. Appl. Phys. **88**, 1855 (2000).
[21]G. Koblmueller, R. Averbeck, L. Geelhaar, H. Riechert, W. Hosler, and P. Pongratz, J. Appl. Phys. **93**, 9591 (2003).
[22]J. Brown, F. Wu, P. M. Petroff, and J. S. Speck, Appl. Phys. Lett. **84**, 690 (2004).
[23]S. Guha, N. A. Bojarczuk, and D. W. Kisker, Appl. Phys. Lett. **69**, 2879 (1996).
[24]K. L. Chopra, *Thin Film Phenomena* (McGraw-Hill, New York, 1969).
[25]I. Barin, *Thermochemical Data of Pure Substances* (VCH, Weinheim, 1993).